Photoproduction of Axionlike Particles

Daniel Aloni,[1,*] Cristiano Fanelli,[2,†] Yotam Soreq,[3,4,‡] and Mike Williams[2,§]

[1]*Department of Particle Physics and Astrophysics, Weizmann Institute of Science, Rehovot 7610001, Israel*
[2]*Laboratory for Nuclear Science, Massachusetts Institute of Technology, Cambridge, Massachusetts 02139, USA*
[3]*Theoretical Physics Department, CERN, CH-1211 Geneva 23, Switzerland*
[4]*Department of Physics, Technion, Haifa 32000, Israel*

We explore the sensitivity of photon-beam experiments to axionlike particles (ALPs) with QCD-scale masses whose dominant coupling to the standard model is either to photons or gluons. We introduce a novel data-driven method that eliminates the need for knowledge of nuclear form factors or the photon-beam flux when considering coherent Primakoff production off a nuclear target, and show that data collected by the PRIMEX experiment in 2004 could improve the sensitivity to ALPs with $0.03 \lesssim m_a \lesssim 0.3$ GeV by an order of magnitude. Furthermore, we explore the potential sensitivity of running the GLUEX experiment with a nuclear target and its planned PRIMEX -like calorimeter. For the case where the dominant coupling is to gluons, we study photoproduction for the first time, and predict the future sensitivity of the GLUEX experiment using its nominal proton target. Finally, we set world-leading limits for both the ALP-gluon coupling and the ALP-photon coupling based on public mass plots.

Axionlike particles (ALPs) are hypothetical pseudoscalars found in many proposed extensions to the standard model (SM), since they naturally address the Strong CP [1–4] and Hierarchy problems [5]. Furthermore, ALPs may explain the muon magnetic moment anomaly [6,7], and could connect SM particles to dark matter by providing a *portal* [8–11]. The couplings of ALPs to the SM are highly suppressed at low energies by a large cutoff scale Λ; however, since ALPs, a, are pseudo-Nambu-Goldstone bosons, their mass (m_a) can be much smaller than the scale that controls their dynamics, i.e., $m_a \ll \Lambda$. Recently, ALPs with MeV-to-GeV scale masses, henceforth QCD scale, have received considerable interest [7,12–23] (see, in addition, Refs. [24–28] for recent ALP reviews).

In this Letter, we explore the discovery potential of photon-beam experiments for ALPs with QCD-scale masses. Specifically, we consider two cases: ALPs whose dominant coupling to SM particles is to photons or to gluons. For the former, the best sensitivity involves coherent Primakoff production off a nuclear target (see Fig. 1, top). While ALP production using the Primakoff process has been studied before [7,29], our Letter is novel in three aspects: (i) we introduce a fully data-driven ALP normalization method, which eliminates the need for

knowledge of nuclear form factors or the photon-beam flux; (ii) we show that data collected by the PRIMEX experiment at Jefferson Lab in 2004 using a Pb target could improve the sensitivity to ALPs with $0.03 \lesssim m_a \lesssim 0.3$ GeV by an order of magnitude on Λ; in fact, we are able to set competitive limits from a diphoton mass plot published in Ref. [30] from a single angular bin; and (iii) we explore for the first time the potential sensitivity of running the GLUEX experiment at Jefferson Lab with a nuclear target and its planned PRIMEX -like calorimeter. For the case where the dominant SM coupling of ALPs is to gluons, we extend our work in Ref. [31] and study photoproduction for the first time. The dominant photoproduction mechanism is
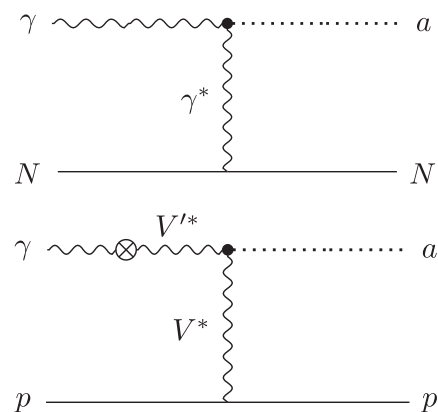

FIG. 1. (top) Primakoff production via t-channel photon exchange, and (bottom) photoproduction via photon–vector-meson mixing and t-channel vector-meson exchange.

photon–vector-meson mixing and t-channel vector-meson exchange (see Fig. 1, bottom). We obtain the future sensitivity of the GLUEX experiment using its nominal proton target, and set world-leading limits based on a public mass plot.

The effective Lagrangian describing the interactions of ALPs with photons and gluons is

$$\mathcal{L}_{\text{eff}} \supset \frac{c_\gamma}{4\Lambda} a F^{\mu\nu} \tilde{F}_{\mu\nu} - \frac{4\pi\alpha_s c_g}{\Lambda} a G^{\mu\nu} \tilde{G}_{\mu\nu}, \qquad (1)$$

where $F_{\mu\nu}(G_{\mu\nu})$ is the photon (gluon) field strength tensor with $\tilde{F}_{\mu\nu} = \frac{1}{2}\epsilon_{\mu\nu\alpha\beta}F^{\alpha\beta}$ ($\tilde{G}_{\mu\nu}$ satisfies a similar expression). Our approach to studying ALP-hadron interactions follows Refs. [32–34], and we take the ALP-pseudoscalar mixing, along with the ALP lifetime and branching fractions, directly from Ref. [31]. The two scenarios considered in this Letter correspond to $c_g = 0$, $c_\gamma = 1$ and $c_g = 1$, $c_\gamma = 0$; however, we stress that our results can be generalized to any other set of ALP couplings to the SM particles (see Ref. [31]).

First, we consider the case where the dominant ALP-SM coupling is to photons. When a photon beam is incident on a nuclear target, the production of pseudoscalars—either the mesons $P = \pi^0$, η or ALPs—at forward angles is dominantly via the coherent Primakoff process for $m_{a,P} \lesssim 1$ GeV. The differential cross section for elastic coherent Primakoff production from a nucleus, N, is given by

$$\frac{d\sigma^{\text{elastic}}_{\gamma N \to aN}}{dt} = \alpha Z_N^2 F_N^2(t) \Gamma_{a\to\gamma\gamma} \mathcal{H}(m_N, m_a, s, t), \qquad (2)$$

where t and s are the Mandelstam variables, F_N is the nuclear form factor (see the Supplemental Material [35] and Refs. [36–38]), $\Gamma_{a\to\gamma\gamma} = c_\gamma^2 m_a^3/(64\pi\Lambda^2)$ is the partial decay width of the decay $a \to \gamma\gamma$, and

$$\mathcal{H}(m_N, m_a, s, t) \equiv 128\pi \frac{m_N^4}{m_a^3}$$
$$\times \frac{m_a^2 t(m_N^2 + s) - m_a^4 m_N^2 - t[(s - m_N^2)^2 + st]}{t^2(s - m_N^2)^2(t - 4m_N^2)^2}.$$
$$(3)$$

For pseudoscalar mesons, the corresponding differential cross section is obtained by the replacement $a \to P$.

For small values of t (forward angles), where elastic coherent Primakoff production is dominant, the nuclear form factor dependence can be canceled by forming the ratio of the ALP and P differential cross sections as follows:

$$\frac{d\sigma^{\text{elastic}}_{\gamma N \to aN}}{dt} = \frac{\Gamma_{a\to\gamma\gamma}}{\Gamma_{P\to\gamma\gamma}} \frac{\mathcal{H}(m_N, m_a, s, t)}{\mathcal{H}(m_N, m_P, s, t)} \frac{d\sigma^{\text{elastic}}_{\gamma N \to PN}}{dt}. \qquad (4)$$

Therefore, the ALP yield—up to a factor of the model parameters $(c_\gamma/\Lambda)^2$—can be determined from the observed π^0 and/or η Primakoff yields, making this a completely data-driven search. The nuclear form factor does not need to be known, and the photon flux also cancels using our approach. A correction must be applied to account for any mass dependence in the detector efficiency at fixed t and s, though this should be easy to obtain from simulation given that the $a \to \gamma\gamma$ decay distribution is known (it must be uniform in the a rest frame). Finally, we note that quasielastic ALP Primakoff production can be estimated using a similar approach; however, this production mechanism is negligible in the m_a range considered here (see the Supplemental Material [35]).

The first run of the PRIMEX experiment was in Hall B at Jefferson Lab in 2004 [30]. Data were collected on both C and Pb targets using a 4.9–5.5 GeV photon beam and a high-resolution multichannel calorimeter, which allowed PRIMEX to make the most precise measurement to date of the $\pi^0 \to \gamma\gamma$ decay width. The integrated luminosities were 1.9/pb for C and 0.14/pb for Pb. A follow-up run of PRIMEX was performed in 2010, which collected 4.3/pb on C and 6.5/pb on Si, though only preliminary results have been produced thus far from this data set.

Reference [30] published the diphoton mass spectrum near the π^0 peak for one small forward angular bin from the C data obtained in the first PRIMEX run (see Fig. 2 of Ref. [30]). This data corresponds to lab-frame angles $0.02° < \theta_{\gamma\gamma} < 0.04°$ and masses $0.1 < m_{\gamma\gamma} < 0.17$ GeV. The diphoton efficiency is roughly constant within such a small angular and mass window; therefore, using the observed π^0 yield in the published peak (≈ 5100) and the background yield at each $m_{\gamma\gamma}$, we can use Eq. (4) to place constraints on Λ for $c_\gamma = 1$ and $c_g = 0$. For example, at $m_a = 0.11$ GeV the background in a $\pm 2\sigma$ window is ≈ 300 giving a rough estimate of the sensitivity to the ALP yield of $\approx 2\sqrt{300}$. Using Eq. (4) we estimate this corresponds to $\Lambda \approx 0.6$ TeV, which is comparable to the world-leading constraint from LEP at this mass [15,39]. In the Supplemental Material [35], we perform a more rigorous study of this spectrum, the results of which are shown in Fig. 2 and confirm that this small fraction of the PRIMEX data sample provides competitive sensitivity to LEP—and even gives world-leading constraints at a few masses.

To estimate the sensitivity of each PRIMEX data sample, i.e., not just the one bin shown in Fig. 2 of Ref. [30], we need to determine the mass dependence of the efficiency and to estimate the background versus $m_{\gamma\gamma}$ in each sample. A detailed description of this part of the analysis is provided in the Supplemental Material [35], and briefly summarized here. We assume that the same selection criteria applied in Ref. [30] are used for the ALP search and take the PRIMEX calorimeter acceptance and resolution from Refs. [45,46]. Furthermore, we assume that the ALP bump hunt will only use candidates with $\theta_{\gamma\gamma} < 0.5°$, where
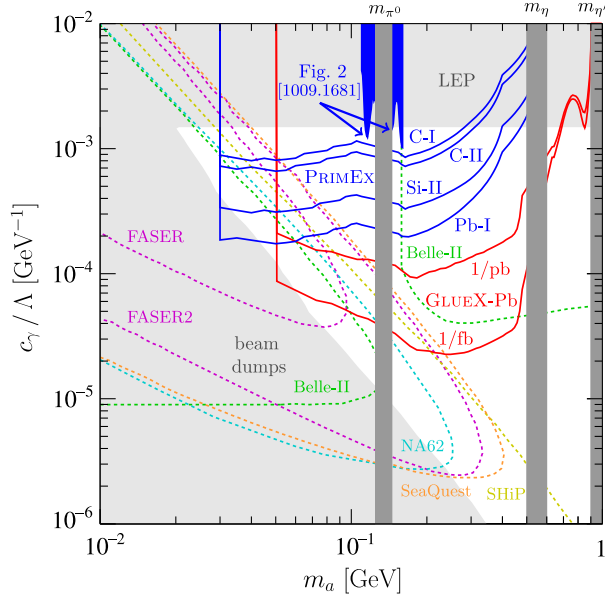
FIG. 2. The PRIMEX (blue) and GLUEX (red) projections for the ALP-photon coupling ($c_\gamma = 1$, $c_g = 0$) compared to the current bounds [15,39–41] and projections of NA62, SeaQuest, Belle 2, SHiP, and FASER [13,42–44]. In addition, a new limit is set (dark blue shaded regions) using the published $m_{\gamma\gamma}$ spectrum from one angular bin of carbon-target PRIMEX data from Fig. 2 of Ref. [30].

π^0 production is dominated by the Primakoff process for all targets.

Using the known nuclear form factors and Primakoff differential cross section [47–49], we generate Primakoff π^0 Monte Carlo events for the PRIMEX photon-beam energy. We require that both photons from the $\pi^0 \to \gamma\gamma$ decay are in the PRIMEX calorimeter fiducial acceptance region [30] and apply the required smearing to account for resolution. The width of our Monte Carlo π^0 peak is consistent with the data in Ref. [30]. We then apply the full selection of Ref. [30] and compare our predicted π^0 Primakoff yields to those of Ref. [30], which are in agreement assuming a reconstruction efficiency of about 90% per photon. We assume that this average per-photon efficiency is independent of the ALP mass in the search region. In addition, we discard the low-m_a region where the photon clusters begin to overlap and the acceptance has strong mass dependence. Lower masses can likely be explored in an analysis of the actual PRIMEX data with access to a full detector simulation.

As in any bump hunt, obtaining a data-driven background estimate is straightforward using the $m_{\gamma\gamma}$ sidebands at each m_a (see, e.g., Refs. [50,51]). However, estimating the background without the data is considerably more difficult, so we adopt a conservative approach. We considered many possible backgrounds, e.g., $\gamma N \to N\omega(\pi^0[\gamma\gamma]\gamma)$ where one photon is not reconstructed or the π^0 photons are merged into a single cluster, though we found that no hadronic reactions are capable of contributing

background at a rate comparable to that observed in Fig. 2 of Ref. [30] in the mass range probed by PRIMEX. Thus, we conclude that the PRIMEX background is dominantly due to electromagnetic interactions of the photon beam with the target that produce either additional photons or e^+e^- pairs. Figure 2 of Ref. [30] shows the forward-most angular bin with a nonneglibile production cross section. Given that the beam backgrounds should decrease moving away from the beam line, using this angular bin—and assuming a uniformly distributed background—provides a conservative background estimate. We also conservatively assume that the background density above (below) the $m_{\gamma\gamma}$ region shown in Fig. 2 of Ref. [30] takes on the value at the upper-most (lower-most) bin of the published $m_{\gamma\gamma}$ spectrum. Finally, we scale the beam-induced background, which is shown for the first C run, by the product of the target radiation length and the number of photons on target for other PRIMEX runs.

Our projected sensitivity for each PRIMEX data sample is shown in Fig. 2. The Pb data from the first PRIMEX run, which provides the best sensitivity, would be an order of magnitude better than LEP for $0.03 \lesssim m_a \lesssim 0.3$ GeV and provide world-leading sensitivity up to about 0.5 GeV. In principle, all PRIMEX runs could be combined, though we do not explore that possibility here. We stress again that the PRIMEX Pb data are already on tape, and is well calibrated and understood. All that is needed is to perform a bump hunt on the forward-angle data in the region dominated by Primakoff production. Following the approach we proposed above, the normalization can be done in a purely data-driven way using the observed π^0 Primakoff yield differentially versus t.

An updated version of the PRIMEX experiment is currently running in Hall D at Jefferson Lab using the GLUEX detector with an additional small-angle calorimeter [52]. This new experiment has the potential to explore higher masses than PRIMEX due to the higher photon-beam energy of 11 GeV and the larger acceptance of the GLUEX forward calorimeter; however, the use of a helium target in the current run makes it less sensitive than PRIMEX for ALPs. There are several proposals for future GLUEX running with heavy nuclear targets [53], so it is interesting to explore the potential sensitivity to ALPs of such runs. Specifically, we consider a Pb target here. We take the GLUEX acceptance, efficiency, and resolution from Refs. [54,55], and the corresponding values for the small-angle calorimeter from Ref. [52]. For $m_a < m_\eta$, we rescale the expected beam background from the PRIMEX Pb run. There are three additional backgrounds that contribute to the GLUEX run at higher masses: Primakoff production of η and η' mesons, and coherent nuclear production of $\gamma N \to N\omega(\pi^0[\gamma\gamma]\gamma)$ (as described above). The cross sections for these processes are well known, making it straightforward to estimate their yields using Monte Carlo calculations.

An additional complication arises when projecting the sensitivity of GLUEX. The GLUEX experiment could explore regions of ALP parameter space where the ALP flight distance becomes non-negligible. Using Monte Carlo calculations, we estimate that the impact on the ALP mass resolution and acceptance is small provided that its lab-frame flight distance is $\lesssim 30$ cm (the length of the nominal liquid hydrogen target cell). For simplicity, we apply a fiducial cut on the flight distance at 30 cm, which is conservative since ALPs that decay after this distance could still be detected and a detailed study could determine the appropriate signal shape for each value of Λ. Our estimate of the projected reach for GLUEX including the PRIMEX -like calorimeter is shown in Fig. 2. The larger data set assumes that as much data is collected as is expected in the full GLUEX proton-target run. The smaller data set corresponds to collecting $\mathcal{O}$ (one month) of Pb-target data at the nominal GLUEX data-taking rate (see the Supplemental Material [35] and Ref. [56]).

Figure 2 shows that Primakoff production using photon beams can provide unique sensitivity to ALPs. The Pb data from PRIMEX, which has been on tape since 2004, could provide an order of magnitude better sensitivity than LEP for $0.03 \lesssim m_a \lesssim 0.3$ GeV. Running the GLUEX experiment for a few years with a Pb target and its PRIMEX -like small-angle calorimeter could explore the remaining parameter space down to where future beam-dump experiments will have sensitivity. Much of this parameter space is not accessible at any other current or proposed future experiment.

We now move on to considering the case where the dominant ALP-SM coupling is to gluons. In this scenario, nuclear targets do not provide a large advantage since both the signal and background scale similarly with the number of nucleons, so we consider the nominal liquid-hydrogen target and default experimental GLUEX setup, which has been running for the past few years. When a photon beam is incident on a proton target, exclusive pseudoscalar production is dominantly via photon–vector-meson mixing as shown in Fig. 1, bottom. In the Supplemental Material [35], we show that—once both π^0 and η photoproduction are well understood—it is possible to derive a fully data-driven normalization strategy similar to the one we proposed above for Primakoff production. As discussed in Ref. [57], η production at GLUEX energies, while clearly dominantly t channel, is not yet fully understood. Therefore, we will adopt a simplified approach below, though we do provide a complete description of how to implement the fully data-driven strategy for future searches in the Supplemental Material [35].

In principle, ALP searches at GLUEX could look for hadronic final states like $a \to 3\pi$ and $a \to \eta\pi\pi$; however, we studied these and found that the mass resolution at GLUEX makes ALP peaks comparable in width to ω, η', $\phi \to 3\pi$ and $\eta', f_2 \to \eta\pi\pi$ making it likely that large mass

regions need to be vetoed in such searches. Furthermore, the sensitivity at higher masses would not be competitive with b-hadron decays [31]. Therefore, we choose to focus on the $a \to \gamma\gamma$ decay in the region between the π^0 and η mesons, where its branching fraction is close to unity and diphoton backgrounds are small. Since $a \to \pi\pi$ and $a \to \pi^0\gamma$ are forbidden by C and CP, respectively, the $a \to \gamma\gamma$ decay is dominant in all ALP models in most of this mass region.

For $m_{\pi^0} < m_a < m_\eta$, the ALP-gluon coupling can be replaced by ALP–pseudoscalar-meson mixing by performing a chiral transformation of the light-quark fields [32–34]. Following Ref. [31], we denote the mixing of the ALP with the π^0 and η as $\langle \mathbf{a\pi^0} \rangle$ and $\langle \mathbf{a\eta} \rangle$, respectively, and we take these m_a-dependent mixings directly from Ref. [31]. For $|t| \lesssim 1$ GeV^2 in this m_a region, at fixed s and t the following approximation is valid to $\mathcal{O}(1)$, which is roughly the same fidelity with which the ALP-pseudoscalar mixing terms are known:

$$\frac{d\sigma_{\gamma p \to ap}}{dt} \approx \left(\frac{f_\pi}{f_a}\right)^2$$
$$\times \left(|\langle \mathbf{a\pi^0} \rangle|^2 \frac{d\sigma_{\gamma p \to \pi^0 p}}{dt} + |\langle \mathbf{a\eta} \rangle|^2 \frac{d\sigma_{\gamma p \to \eta p}}{dt}\right), \quad (5)$$

where f_π and $f_a = \Lambda/(32\pi^2 c_g)$ are the pion and ALP decay constants. This approximation works well in this mass range due to the dominance of the contributions from π^0 or η mixing to the ALP $U(3)$ representation. We adopt the relevant numerical values from Refs. [58–60], see Supplemental Material [35] for details.

Reference [57] published the $m_{\gamma\gamma}$ spectrum, along with the yields and efficiencies versus t of both the π^0 and η mesons. In the Supplemental Material, we perform a bump hunt of the $m_{\gamma\gamma}$ spectrum to obtain upper limits on the ALP yield at each m_a. The expected ALP yield in a small bin of $[s, t]$ is related to Λ (or f_a) using Eq. (5) according to

$$n_a(s, t) \approx \left(\frac{f_\pi}{f_a}\right)^2 \left[|\langle \mathbf{a\pi^0} \rangle|^2 \frac{n_{\pi^0}(s, t)\epsilon(m_a, s, t)}{\mathcal{B}(\pi^0 \to \gamma\gamma)\epsilon(m_\pi, s, t)}\right.$$
$$\left. + |\langle \mathbf{a\eta} \rangle|^2 \frac{n_\eta(s, t)\epsilon(m_a, s, t)}{\mathcal{B}(\eta \to \gamma\gamma)\epsilon(m_\eta, s, t)}\right] \mathcal{B}(a \to \gamma\gamma), \quad (6)$$

where ϵ denotes the product of the detector acceptance and efficiency. We linearly interpolate the efficiencies given in Ref. [57] at m_{π^0} and m_η for m_a, and confirm this approach is valid to $\mathcal{O}(10\%)$ using toy Monte Carlo calculations as described in the Supplemental Material [35] (additionally, the same ALP lifetime correction is applied here, though this is a small correction). The total expected ALP yield is simply the sum of $n_a(s, t)$ over all bins. By comparing the expected ALP yields to the upper limits obtained from the bump hunt of the $m_{\gamma\gamma}$ spectrum, we place constraints on c_g/Λ (see Fig. 3). These limits are the best over most of the
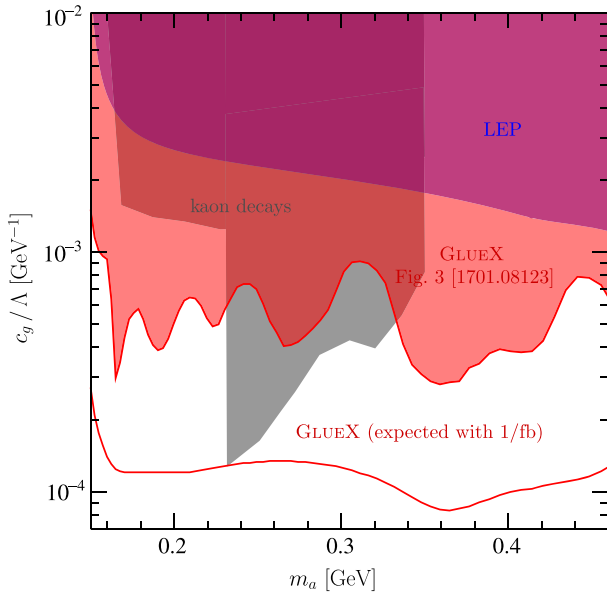
FIG. 3. The GLUEX projection for the ALP-gluon coupling ($c_\gamma = 0$, $c_g = 1$) compared to the current bounds [31] from LEP [15,39] and kaon decays [14,61–63]. In addition, a new limit is set using the published $m_{\gamma\gamma}$ spectrum from $\approx 1/$pb of GLUEX data from Fig. 3 of Ref. [57].

$0.15 < m_a < 0.46$ GeV region. Finally, we also provide the expected sensitivity from a 1/fb GLUEX data set, which is substantially better than any existing limits over most of this mass region.

In summary, we explored the sensitivity of photon-beam experiments to ALPs with QCD-scale masses whose dominant coupling is to either photons or gluons. For the photon-dominant coupling scenario, we introduced a novel data-driven method that eliminates the need for knowledge of nuclear form factors or the photon-beam flux when considering coherent Primakoff production off of a nuclear target, and showed that data collected by PRIMEX in 2004 could improve the sensitivity to ALPs with $0.03 \lesssim m_a \lesssim 0.3$ GeV by an order of magnitude. We also explored the potential sensitivity of running the GLUEX experiment with a nuclear target. For the case where the dominant coupling is to gluons, we studied photoproduction for the first time, and predicted the future sensitivity of the GLUEX experiment using its nominal proton target. For both scenarios, we set world-leading limits based on public mass plots.

*daniel.aloni@weizmann.ac.il
†cfanelli@mit.edu
‡yotam.soreq@cern.ch
§mwill@mit.edu

[1] R. D. Peccei and H. R. Quinn, *CP* Conservation in the Presence of Instantons, Phys. Rev. Lett. **38**, 1440 (1977).

[2] R. D. Peccei and H. R. Quinn, Constraints imposed by *CP* conservation in the presence of instantons, Phys. Rev. D **16**, 1791 (1977).

[3] S. Weinberg, A New Light Boson?, Phys. Rev. Lett. **40**, 223 (1978).

[4] F. Wilczek, Problem of Strong *P* and *T* Invariance in the Presence of Instantons, Phys. Rev. Lett. **40**, 279 (1978).

[5] P. W. Graham, D. E. Kaplan, and S. Rajendran, Cosmological Relaxation of the Electroweak Scale, Phys. Rev. Lett. **115**, 221801 (2015).

[6] D. Chang, W.-F. Chang, C.-H. Chou, and W.-Y. Keung, Large two loop contributions to g-2 from a generic pseudoscalar boson, Phys. Rev. D **63**, 091301(R) (2001).

[7] W. J. Marciano, A. Masiero, P. Paradisi, and M. Passera, Contributions of axionlike particles to lepton dipole moments, Phys. Rev. D **94**, 115033 (2016).

[8] Y. Nomura and J. Thaler, Dark matter through the axion portal, Phys. Rev. D **79**, 075008 (2009).

[9] M. Freytsis and Z. Ligeti, On dark matter models with uniquely spin-dependent detection possibilities, Phys. Rev. D **83**, 115009 (2011).

[10] M. J. Dolan, F. Kahlhoefer, C. McCabe, and K. Schmidt-Hoberg, A taste of dark matter: Flavour constraints on pseudoscalar mediators, J. High Energy Phys. 03 (2015) 171; Erratum, J. High Energy Phys. 07 (2015) 103(E).

[11] Y. Hochberg, E. Kuflik, R. Mcgehee, H. Murayama, and K. Schutz, SIMPs through the axion portal, Phys. Rev. D **98**, 115031 (2018).

[12] J. Jaeckel and M. Spannowsky, Probing MeV to 90 GeV axion-like particles with LEP and LHC, Phys. Lett. B **753**, 482 (2016).

[13] B. Dbrich, J. Jaeckel, F. Kahlhoefer, A. Ringwald, and K. Schmidt-Hoberg, ALPtraum: ALP production in proton beam dump experiments, J. High Energy Phys. 02 (2016) 018.

[14] E. Izaguirre, T. Lin, and B. Shuve, Searching for Axionlike Particles in Flavor-Changing Neutral Current Processes, Phys. Rev. Lett. **118**, 111802 (2017).

[15] S. Knapen, T. Lin, H. K. Lou, and T. Melia, Searching for Axionlike Particles with Ultraperipheral Heavy-Ion Collisions, Phys. Rev. Lett. **118**, 171801 (2017).

[16] A. Mariotti, D. Redigolo, F. Sala, and K. Tobioka, New LHC bound on low-mass diphoton resonances, Phys. Lett. B **783**, 13 (2018).

[17] M. Bauer, M. Neubert, and A. Thamm, Collider probes of axion-like particles, J. High Energy Phys. 12 (2017) 044.

[18] X. Cid Vidal, A. Mariotti, D. Redigolo, F. Sala, and K. Tobioka, New axion searches at flavor factories, J. High Energy Phys. 01 (2019) 113.

[19] M. Bauer, M. Heiles, M. Neubert, and A. Thamm, Axion-like particles at future colliders, Eur. Phys. J. C **79,** 74 (2019).

[20] L. Harland-Lang, J. Jaeckel, and M. Spannowsky, A fresh look at ALP searches in fixed target experiments, Phys. Lett. B **793,** 281 (2019).

[21] J. Ebadi, S. Khatibi, and M. Mohammadi Najafabadi, New probes for axion-like particles at hadron colliders, arXiv:1901.03061.

[22] K. Mimasu and V. Sanz, ALPs at colliders, J. High Energy Phys. 06 (2015) 173.

[23] I. Brivio, M. B. Gavela, L. Merlo, K. Mimasu, J. M. No, R. del Rey, and V. Sanz, ALPs effective field theory and collider signatures, Eur. Phys. J. C **77,** 572 (2017).

[24] R. Essig *et al.*, Working Group Report: New light weakly coupled particles, arXiv:1311.0029.

[25] D. J. E. Marsh, Axion cosmology, Phys. Rep. **643,** 1 (2016).

[26] P. W. Graham, I. G. Irastorza, S. K. Lamoreaux, A. Lindner, and K. A. van Bibber, Experimental searches for the axion and axion-like particles, Annu. Rev. Nucl. Part. Sci. **65,** 485 (2015).

[27] I. G. Irastorza and J. Redondo, New experimental approaches in the search for axion-like particles, Prog. Part. Nucl. Phys. **102,** 89 (2018).

[28] J. Beacham *et al.*, Physics Beyond Colliders at CERN: Beyond the Standard Model Working Group Report, arXiv:1901.09966.

[29] A. Gasparian, Search for Hidden Sector Scalar Bosons in $X \rightarrow \gamma\gamma$ Channel with Intense Medium Energy Electron Beams, 2013, https://axion-wimp2013.desy.de/e201031/e212848/Gasparian.pdf. 9th PATRAS 2013 workshop, DESY, Hamburg, Germany.

[30] I. Larin *et al.* (PrimEx Collaboration), A New Measurement of the π^0 Radiative Decay Width, Phys. Rev. Lett. **106,** 162303 (2011).

[31] D. Aloni, Y. Soreq, and M. Williams, Coupling QCD-Scale Axionlike Particles to Gluons, Phys. Rev. Lett. **123,** 031803 (2019)..

[32] H. Georgi, D. B. Kaplan, and L. Randall, Manifesting the invisible axion at low-energies, Phys. Lett. **169B,** 73 (1986).

[33] W. A. Bardeen, R. D. Peccei, and T. Yanagida, Constraints on variant axion models, Nucl. Phys. **B279,** 401 (1987).

[34] L. M. Krauss and M. B. Wise, Constraints on shortlived axions from the decay $\pi^+ \rightarrow e^+ e^- e^+$ neutrino, Phys. Lett. B **176,** 483 (1986).

[35] See the Supplemental Material at http://link.aps.org/supplemental/10.1103/PhysRevLett.123.071801 for technical details of our calculations and the limit-setting procedures used.

[36] D. R. Yennie, M. M. Lévy, and D. G. Ravenhall, Electromagnetic structure of nucleons, Rev. Mod. Phys. **29,** 144 (1957).

[37] L. N. Hand, D. G. Miller, and R. Wilson, Alternative Nucleon Form Factors, Phys. Rev. Lett. **8,** 110 (1962).

[38] M. Tanabashi *et al.* (Particle Data Group Collaboration), Review of particle physics, Phys. Rev. D **98,** 030001 (2018).

[39] G. Abbiendi *et al.* (OPAL Collaboration), Multiphoton production in e^+e^--collisions at s * *(1/2) = 181-GeV to 209-GeV, Eur. Phys. J. C **26,** 331 (2003).

[40] J. D. Bjorken, S. Ecklund, W. R. Nelson, A. Abashian, C. Church, B. Lu, L. W. Mo, T. A. Nunamaker, and P. Rassmann, Search for neutral metastable penetrating particles produced in the SLAC beam dump, Phys. Rev. D **38,** 3375 (1988).

[41] J. Blümlein *et al.*, Limits on neutral light scalar and pseudoscalar particles in a proton beam dump experiment, Z. Phys. C **51,** 341 (1991).

[42] J. L. Feng, I. Galon, F. Kling, and S. Trojanowski, Axionlike particles at FASER: The LHC as a photon beam dump, Phys. Rev. D **98,** 055021 (2018).

[43] A. Berlin, S. Gori, P. Schuster, and N. Toro, Dark sectors at the Fermilab SeaQuest Experiment, Phys. Rev. D **98,** 035011 (2018).

[44] M. J. Dolan, T. Ferber, C. Hearty, F. Kahlhoefer, and K. Schmidt-Hoberg, Revised constraints and Belle II sensitivity for visible and invisible axion-like particles, J. High Energy Phys. 12 (2017) 094.

[45] M. Kubantsev, I. Larin, and A. Gasparian, Performance of the primex electromagnetic calorimeter, in AIP Conf. Proc. **867,** 51 (2006).

[46] I. Larin, D. McNulty, E. Clinton, P. Ambrozewicz, D. Lawrence, I. Nakagawa, Y. Prok, A. Teymurazyan, A. Ahmidouch, A. Asratyan *et al.*, New Measurement of the $\pi0$ Radiative Decay Width, Phys. Rev. Lett. **106,** 162303 (2011).

[47] T. W. Donnelly, J. A. Formaggio, B. R. Holstein, R. G. Milner, and B. Surrow, *Foundations of Nuclear and Particle Physics* (Cambridge University Press, Cambridge, England, 2017).

[48] W. M. Alberico, A. Molinari, T. W. Donnelly, E. L. Kronenberg, and J. W. Van Orden, Scaling in electron scattering from a relativistic Fermi gas, Phys. Rev. C **38,** 1801 (1988).

[49] C. W. De Jager, H. De Vries, and C. De Vries, Nuclear charge-density-distribution parameters from elastic electron scattering, Atom. Data Nucl. Data Tabl. **36,** 495 (1974); Erratum, Atom. Data Nucl. Data Tabl. **16,** 580(E) (1975).

[50] M. Williams, Searching for a particle of unknown mass and lifetime in the presence of an unknown non-monotonic background, J. Instrum. **10,** P06002 (2015).

[51] M. Williams, A novel approach to the bias-variance problem in bump hunting, J. Instrum. **12,** P09034 (2017).

[52] A. Gasparian *et al.*, *Proceedings of the XI International Conference on Calorimetry in Particle Physics* (World Scientific, Singapore, 2004), pp. 109–115.

[53] M. Dugger *et al.*, Probing QCD in the nuclear medium with real photons and nuclear targets at GlueX (2017), https://www.jlab.org/exp_prog/proposals/17/PR12-17-007.pdf.

[54] T. Beattie *et al.*, Construction and performance of the barrel electromagnetic calorimeter for the GlueX experiment, Nucl. Instrum. Methods Phys. Res., Sect. A **896,** 24 (2018).

[55] J. M. Hardin, Upgrading particle identification and searching for leptophobic bosons at GlueX. Ph. D. thesis, Massachusetts Institute of Technology, 2018.

[56] M. Dugger *et al.* (GlueX Collaboration), A study of meson and baryon decays to strange final states with GlueX in Hall D (A proposal to the 39th Jefferson Lab Program Advisory Committee), arXiv:1210.4508.

[57] H. Al Ghoul *et al.* (GlueX Collaboration), Measurement of the beam asymmetry Σ for π^0 and η photoproduction on the proton at $E_\gamma = 9$ GeV, Phys. Rev. C **95,** 042201 (2017).

[58] T. Fujiwara, T. Kugo, H. Terao, S. Uehara, and K. Yamawaki, Nonabelian anomaly and vector mesons as dynamical gauge bosons of hidden local symmetries, Prog. Theor. Phys. **73,** 926 (1985).

[59] R. Machleidt, K. Holinde, and C. Elster, The Bonn meson exchange model for the nucleon nucleon interaction, Phys. Rep. **149,** 1 (1987).

[60] V. Mathieu, G. Fox, and A. P. Szczepaniak, Neutral pion photoproduction in a Regge model, Phys. Rev. D **92,** 074013 (2015).

[61] C. Lazzeroni *et al.* (NA62 Collaboration), Study of the $K^\pm \to \pi^\pm \gamma\gamma$ decay by the NA62 experiment, Phys. Lett. B **732,** 65 (2014).

[62] E. Abouzaid *et al.* (KTeV Collaboration), Final results from the KTeV Experiment on the decay $K_L \to \pi^0 \gamma\gamma$, Phys. Rev. D **77,** 112004 (2008).

[63] S. Gori, G. Perez, and K. Tobiaka noted that an additional bound can be derived from $K^+ \to \pi^+\pi^0$ followed by a-π^0 mixing. We have derived this bound taking $\langle \mathbf{a}\boldsymbol{\pi^0} \rangle$ from Ref. [31] and using the kaon-decay data as in Refs. [14,54].